NANO LETTERS

pubs.acs.org/NanoLett

Controllable N-Doping of Graphene

Beidou Guo,[†,‡] Qian Liu,[†] Erdan Chen,[†] Hewei Zhu,[†] Liang Fang,[‡] and Jian Ru Gong*[,†]

[†]Laboratory for Nanodevices, National Center for Nanoscience and Technology, China, 11 Zhongguancun Beiyitiao, Beijing 100190, People's Republic of China, and [‡]Department of Applied Physics, Chongqing University, Chongqing 400044, People's Republic of China

ABSTRACT Opening and tuning an energy gap in graphene are central to many electronic applications of graphene. Here we report N-doped graphene obtained by NH_3 annealing after N^+-ion irradiation of graphene samples. First, the evolution of the graphene microstructure was investigated following N^+-ion irradiation at different fluences using Raman spectroscopy, showing that defects were introduced in plane after irradiation and then restored after annealing in N_2 or in NH_3. Auger electron spectroscopy (AES) of the graphene annealed in NH_3 after irradiation showed N signal, however, no N signal was observed after annealing in N_2. Last, the field-effect transistor (FET) was fabricated using N-doped graphene and monitored by the source−drain conductance and back-gate voltage ($G_{sd}-V_g$) curves in the measurement. The transport property changed compared to that of the FET made by intrinsic graphene, that is, the Dirac point position moved from positive V_g to negative V_g, indicating the transition of graphene from p-type to n-type after annealing in NH_3. Our approach, which provides a physical mechanism for the introduction of defect and subsequent hetero dopant atoms into the graphene material in a controllable fashion, will be promising for producing graphene-based devices for multiple applications.

KEYWORDS Graphene, N-doping, NH_3 annealing, ion irradiation, Raman spectroscopy, field-effect transistor

Graphene, a two-dimensional (2D) network of sp^2-hybridized carbon atoms packed into hexagonal structure, is a basic building block for graphitic materials of all other dimensionalities. Since long-range π-conjugation in graphene yields extraordinary thermal,[1] mechanical,[2] and electrical properties,[3,4] an enormous effort has been devoted to exploration of its many applications in nanoelectronics, materials science, condensed-matter physics, and low-dimensional physics.[5] However, most electronic applications are handicapped by the absence of a bandgap in the intrinsic material.[6,7] In the quest to opening and tuning an energy gap in graphene, various approaches have been developed to improve the semiconducting properties, exemplified by forming confined geometries of quantum dots,[8] nanoribbons[9,10] and nanomesh,[11] or binding graphene to particular substrates.[12−14] One of the most feasible methods to control the semiconducting properties of graphene is by doping, which is a process intentionally used to tailor the electrical properties of intrinsic semiconductors. The dopant atoms can modify the electronic band structure of graphene, and open up an energy gap between the valence and conduction bands. The semiconducting graphenes by substituting C atoms with B and N atoms were reported through chemical doping, such as chemical vapor deposition (CVD) and electrothermal reactions.[15−17] Nevertheless each of the approaches has its own downside, for instance, realization of binding graphene to certain substrates is very difficult and controversial, the magnitude of a nanoribbon gap is hard to control as it critically depends on the atomic-scale edge of the ribbon, and multilayer-graphene is common in the CVD method.

Ion irradiation has been used for doping in graphite, carbon nanotube (CNT),[18−20] but for graphene, only defect, surface charge and electronic structure after ion irradiation were investigated.[21−23] As we know, pristine graphene has perfect honeycomb structure, and it is difficult to introduce hetero atoms into graphene and control the electrical properties of graphene. In this letter, controllable N-doping in graphene was realized by NH_3 annealing after ion irradiation. In addition, to the best of our knowledge it is the first reported n-type graphene-based field-effect transistor (FET) fabricated at room temperature by this method.

Electrical characteristics of graphene are linked to the quality of the 2D crystal structure,[24,25] therefore it is necessary to investigate the effect of irradiation and annealing on the microstructure of graphene for further understanding the fundamental physics of the process. As a powerful tool for monitoring the process of irradiation and characterizing the properties of graphene,[21,26] Raman spectroscopy (with 514 nm excitation) was used as a main means for the analysis of graphene samples used in the experiment. Otherwise, Raman measurement is also nondestructive, fast, high-resolution, and gives the maximum structural and electronic information.[24,27,28]

Since it is more useful to get *n*-type graphene compared to the easily obtained p-typed graphene by adsorbates,[17] we chose N, the natural candidate because of its similar atomic size as that of C and of its electron donor character for N-doping in graphene. To achieve this goal, we carried out N^+-ion irradiation at room temperature in the vacuum

* To whom correspondence should be addressed. E-mail: gongjr@nanoctr.cn.
Received for review: 08/31/2010
Published on Web: 10/22/2010

DOI: 10.1021/nl103079j | *Nano Lett.* **2010,** *10,* 4975–4980

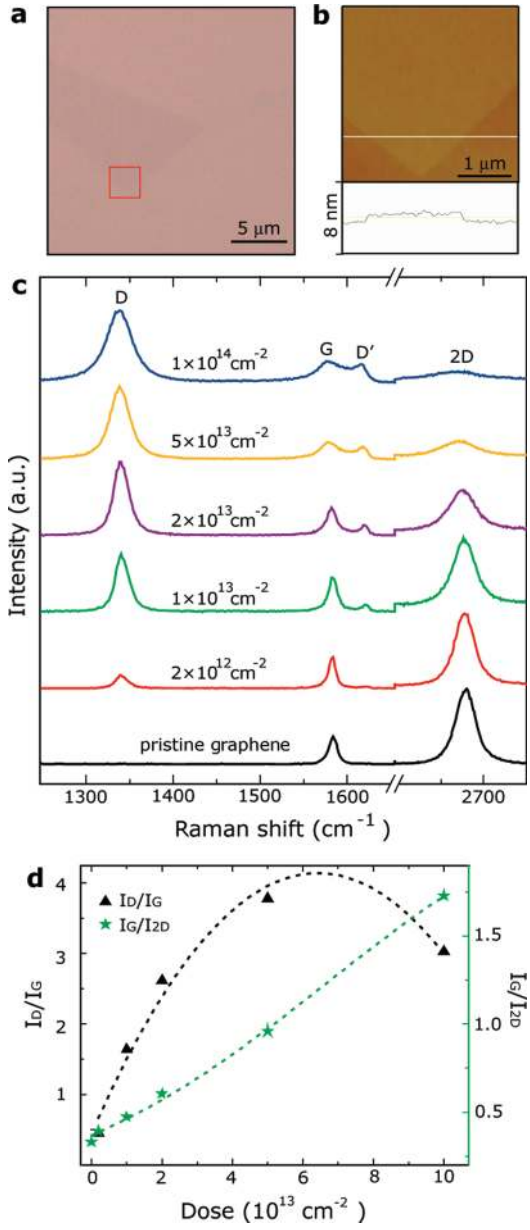

FIGURE 1. (a) The optical image of the mechanical exfoliated single-layer pristine graphene on the 300 nm $SiO_2/p^{2+}Si$ substrate. (b) The AFM image recorded in the red square of (a) with the cross-section analysis. (c) Raman spectra for various fluences of N^+-ions implanted into the same graphene sample. (d) Summary of the ratio of I_G/I_{2D} and I_D/I_G relative to the irradiation dose.

chamber on the mechanical exfoliated single-layer pristine graphene on the 300 nm $SiO_2/p^{2+}Si$ substrate, and the single layer was confirmed by the optical (Figure 1a) and AFM (Figure 1b, the vertical distance of ca. 0.7 nm is shown in the cross-section analysis) images and the Raman spectrum of the pristine graphene (Figure 1c, black curve, $I_{2D}/I_G > 3$).[9,29]

Then, the graphene was irradiated with 30 keV N^+-ions at five different fluences: 2×10^{12}, 1×10^{13}, 2×10^{13}, 5×10^{13}, 1×10^{14} cm^{-2}, and the corresponding Raman spectra are plotted in Figure 1c. The spectra show three main features in the 1000−3000 cm^{-1} region. For the pristine graphene, the D peak does not show, indicating the high quality of the crystal lattice. As graphene is exposed to N^+-ions, the D peak, a signature for disorder at ∼1345 cm^{-1}, and the weak D′ band at ∼1620 cm^{-1} considered another Raman feature induced by defects appear, displaying the increase of defects with the increasing exposure doses. The intensity of 2D band at ∼2675 cm^{-1}, corresponding to the overtone of the D band,[21] decreases by increasing the fluence of ion irradiation, and the ratio of I_G/I_{2D} shows a linear increase with the increasing dose as shown in Figure 1c (green). The evolution of the aforementioned Raman spectra of graphene indicates that the disorder increases with the increase of the N^+-ion irradiation fluence.

The diagram of the ratio of I_D/I_G relative to the irradiation dose is plotted in Figure 2d (black). The ratio of I_D/I_G increases with the increasing fluence, then drops after reaching the highest value. The highest value of the curve is taken as a boundary between the first and second stage of disorder. In the first stage, a proper quantification of the amount of defects in graphene has been given by the well-known Tuinstra−Koenig (TK)[30] relation, $L_a = (2.4 \times 10^{-10})\lambda^4(I_D/I_G)^{-1}$. Here L_a is the size of in-plane crystallites formed by a certain number of carbon rings and λ is the laser excitation wavelength.[21,24,26,30] It can be assumed that the higher the number of defects with the increasing irradiation fluence, the higher the D peak intensity, and the smaller L_a. While in the second stage, the TK relation was broken down as $I_D/I_G \propto L_a^2$.[24] The above relations can be used to determine which stage the graphene is in.

With the increase of the irradiation fluences, the microscopic structural properties of graphene will undergo a very important sequence of regimes: graphene-nanocrystalline graphene-low sp^3 amorphous graphene-high sp^3 amorphous carbon. The above three-stage classification of disorder allows to simply assess all the Raman spectra of carbons.[20,21,24,31] At the first two stages, annealing at an appropriate temperature is able to restore the primitive order mostly.[20,31] Therefore, the careful choice of a maximal threshold fluence is needed for the sake of restoration of the graphene structure after annealing. Considering the downshift of G band with the increasing fluence, the graphene irradiated with fluences at 1×10^{14} cm^{-2} in our experiment would be located at the beginning of the second stage, thus, the formation of amorphous carbon was avoided.

The Raman spectra display that the intensity of the D peak induced by irradiation is significantly reduced by postannealing in N_2 (see Figure S1 in Supporting Information), indicating the restoration of the damaged lattice, that is, the irradiated graphene with the sp^3-like bonds or other vacancy defects would be changed into sp^2-bonded graphene after postannealing in N_2. When increasing the temperature, the ratio of I_D/I_G decreases. The change of the annealing time causes little change of the I_D/I_G ratio, showing that the annealing time in our experiment is not the main factor for

DOI: 10.1021/nl103079j | Nano Lett. 2010, 10, 4975–4980

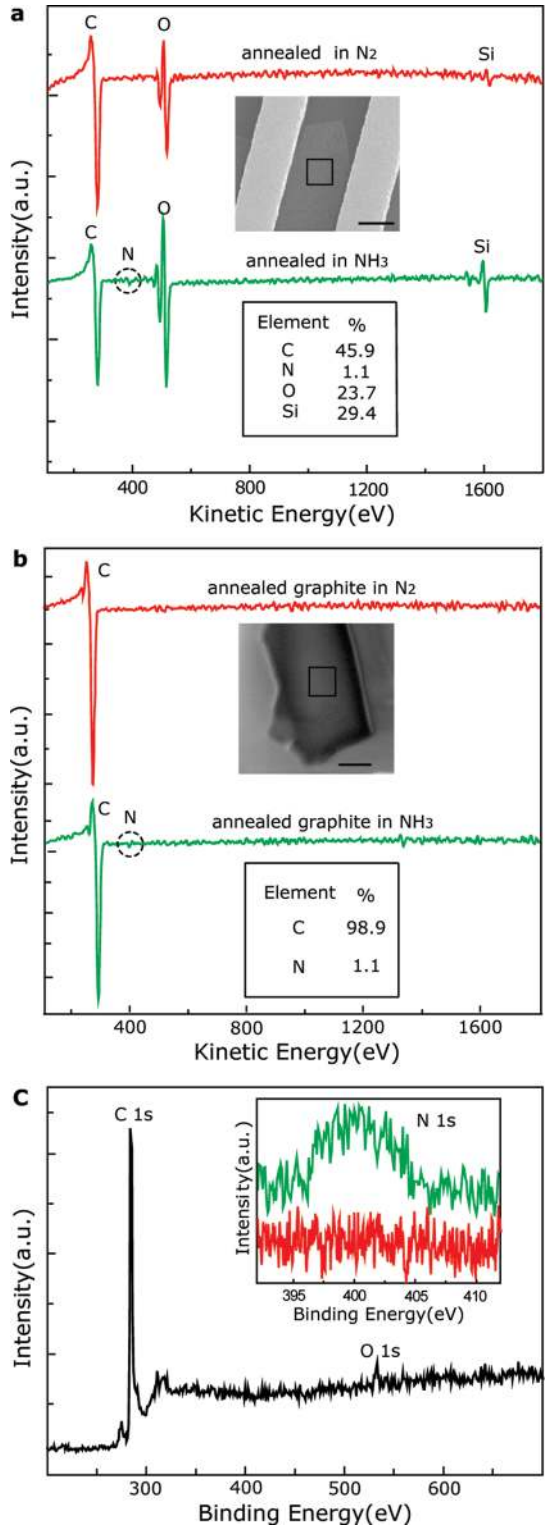

FIGURE 2. (a) AES data of the graphene annealed in N_2 (red) and in NH_3 (green) at 1100 °C for 30s, respectively. (b) AES data of the graphite annealed in N_2 (red) and in NH_3 (green) at the same conditions as that for graphene. Insets: The AES detecting regions marked by the square in the SEM images and the atomic concentration. The scale bar is 1 μm. (c) The representative full spectrum of XPS for graphite annealed in N_2 and in NH_3 after irradiation. Inset is the XPS N 1s spectra: (red) annealed in N_2, (green) annealed in NH_3.

affecting the restoration of defects in the irradiated graphene, and the similar result was obtained for the graphite sample (see Table S1 in Supporting Information).[20] The irradiated graphene still keeps stable when postannealing up to the tested 1100 °C. After optimizing the annealing time and temperature, the largest upshift, minimal full width at half maximum (fwhm) of G band, the lowest ratio of I_{2D}/I_G, and the minimal intensity ratio of $I_D/I_G \sim 0.32$, representing the maximal extent of restoration of defects, are obtained at the experimental condition of 1100 °C for 30 s.

Auger electron spectroscopy (AES) is an invaluable technique for chemical analysis of nanostructured materials and thin films. The spectra of AES (PHI-700 scanning auger nanoprobe) for the surface elemental analysis show no N signal in graphene after irradiation and postannealing in N_2 (Figure 2a, red), indicating that the N atomic concentration is too low to be detected by AES, or there is no N element in graphene after annealing in N_2. Therefore, most of the defects introduced by irradiation would be vacancy defects.[32] For N-doping of graphene, NH_3 annealing was performed at 1100 °C for 30s after irradiation. AES result shows N signal locating at ~400 eV (Figure 2a, green), confirming the N-doping of graphene.

To further prove the NH_3 effect on the N-doping, the graphite flakes annealed in N_2 and in NH_3 at the same conditions as that for graphene were also measured by AES (Figure 2b) for a control experiment. Same as the result of graphene, there is no N signal in the graphite flake after annealed in N_2, but the N signal is detected after annealing in NH_3, which indicates that the doping of the graphite is not introduced by the irradiated N^+ ions which might exist either in the graphite or in the substrate at the irradiation fluence used in our experiment. In addition, we annealed the pristine graphene in NH_3 under the identical conditions with that for the irradiated graphene and no N signal was observed. Our result is consistent with the previous report that the physisorbed NH_3 could be removed from the graphene surface by pumping[17] and NH_3 completely desorbed from the pristine CNTs above 140 K.[33] It should be noted that the O and Si signals appearing in the graphene sample come from the SiO_2 on the substrate surface because the electron of AES can reach the substrate across the one-atom thick graphene and no O and Si signals are observed in the graphite sample treated under the same conditions as that for the graphene.

The N-doping was also characterized by X-ray photoelectron spectroscopy (XPS, ESCA Lab220I-XL) on the graphite flake. The representative full spectrum of XPS for samples annealed in N_2 and in NH_3 is shown in Figure 2c, and no obvious difference is observed. But, the XPS N 1s spectra are dramatically different as displayed in the inset; the sample annealed in NH_3 after irradiation shows distinguished N signal. In contrast, the N signal for the sample annealed in N_2 after irradiation is not observable. The above

DOI: 10.1021/nl103079j | *Nano Lett.* **2010,** *10,* 4975–4980

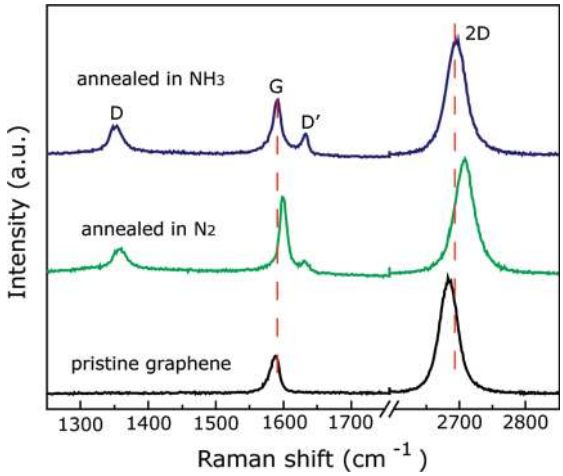

FIGURE 3. Raman spectra of the pristine (black) and irradiated graphene after annealing in N_2 (green) and in NH_3 (blue). The spectra of the annealed graphene upshift relative to that of the pristine graphene, and the shift is more obvious for that in N_2 compared to that in NH_3.

result verifies the N-doping effect in NH_3 after irradiation, which is consistent with the AES data.

Considering strain and tension of the graphene structure caused by the recovery of defects after annealing in N_2, the bands of Raman spectra upshift (Figure 3). The D band shifts $\sim$19 cm^{-1}, while G band shifts $\sim$15 cm^{-1}, and 2D band shifts $\sim$28 cm^{-1} after N_2 annealing at 1100 °C for 30 s relative to that of pristine graphene. However, the vacancy defects of the irradiated graphene are repaired with N atoms after annealing in NH_3 since the C−N bond formation occur predominantly on the defect sites in the plane, where the C atoms are much more chemically reactive than that in the plane of the perfect graphene.[17,34] According to the previous report,[35] the C−N bond internuclear distance is 0.134 nm and for the next neighbor C−C bonds a distance of 0.138 nm. Both of these values are only a little shorter than the C−C graphene distance of 0.14 nm, therefore, a torsion of 0.3 degrees was formed around C−N bonds. It suggests that the structural tension and strain of graphene cause the more prominent spectra upshift of the graphene annealed in N_2 after irradiation compared to that of the irradiated graphene after annealing in NH_3.[35,36] On the other hand, the mode at $\sim$1620 cm^{-1}, termed as D′ denoting disorder, becomes more prominent after annealing in NH_3 than in N_2, which might be caused by hetero N atoms.[37,38]

To investigate the electronic properties of different graphene samples, the graphene-based back-gate FETs were fabricated on a 300 nm $SiO_2/p^{2+}Si$ substrate and the source/drain electrodes were defined by electron beam lithography and thermal metal deposition of Cr/Au (5 nm/70 nm)[39,40] as shown by the scheme and SEM image in Figure 4a.

The source−drain conductance and back-gate voltage ($G_{sd}-V_g$) curves of the pristine graphene FET measured in air and in vacuum (Figure 4b) show bipolar transistor effect, and the minimal conduction corresponds to the Dirac point

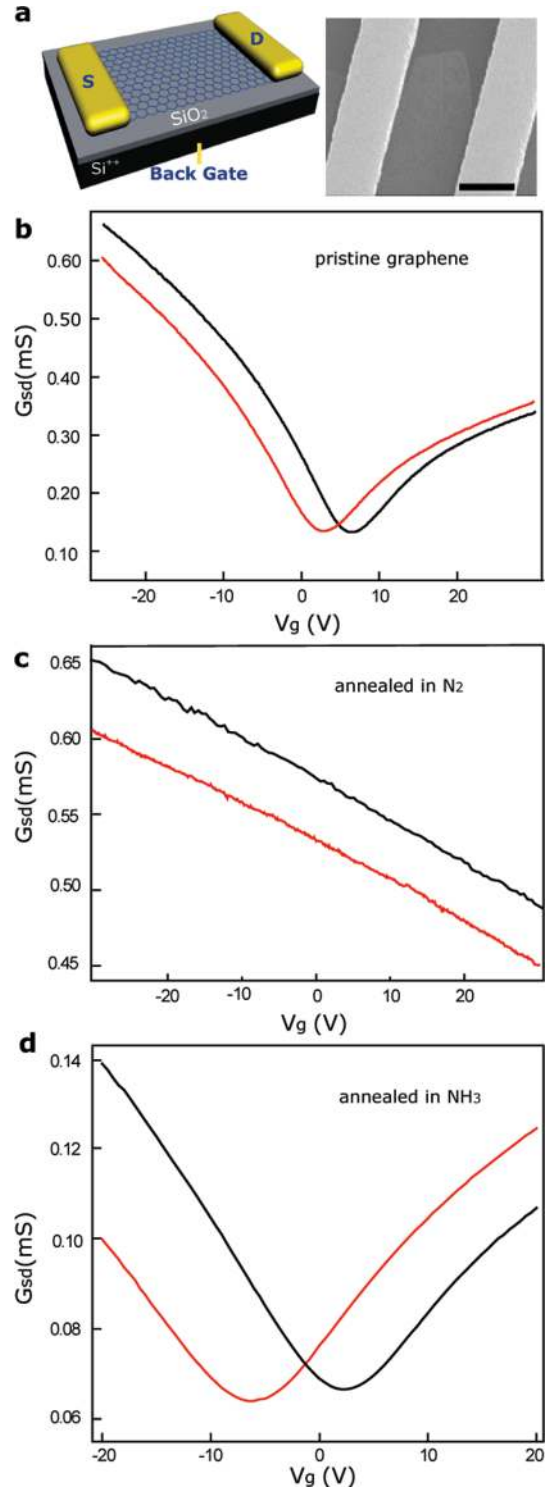

FIGURE 4. Comparison of the transport property of FET using different graphene samples (black and red curves were measured in air and in vacuum, respectively). (a) The scheme of the graphene-based FET device (left) and a typical SEM image of the device (right). The scale bar is 1 μm. (b) The $G_{sd}-V_g$ curves of the pristine graphene. (c) The $G_{sd}-V_g$ curves of the graphene annealed in N_2 after irradiation. (d) The $G_{sd}-V_g$ curves of graphene annealed in NH_3 after irradiation. $G_{sd}-V_g$ curves in (b−d) are measured at $V_{sd} = 0.03$ V.

DOI: 10.1021/nl103079j | Nano Lett. 2010, 10, 4975–4980

(V_{dirac}). When $V_g < V_{dirac}$, it operates as a p-channel FET, and for $V_g > V_{dirac}$, the device operate as an n-channel FET.[30] Therefore, the V_{dirac} locating at the positive gate voltage indicates the p-type hole doping behavior of pristine graphene due to doping of the physisorbed molecular oxygen.[15,18,30] For the graphene annealed in N_2 after irradiation, it shows obvious p-type doping due to the defects and the physisorbed oxygen molecules,[17] and the bipolar transistor effect disappeared (Figure 4c).

In our transport measurement, the graphene annealed in NH_3 after irradiation shows distinguishing transport features both in vacuum and in air (Figure 4d) compared with the pristine graphene FET and the FET with the graphene annealed in N_2. In vacuum, the graphene FET displays intrinsic clear n-type behavior with the Dirac point at the negative gate voltage, showing N-doping in graphene. Pumping in vacuum reduces the hole conduction and enhances the electron conduction, which corresponds to a decrease in p-type doping caused by partial physical adsorption. Because of the adsorption of oxygen molecule in air, the hole and electron conduction change at the different V_g and the minimal conduction locates at the positive V_g.[17] (See more transport data in Figure S2 of Supporting Information). The carrier mobility (μ) can be deduced by $\mu = L/WC_gV_{sd})(\Delta I_{sd}/\Delta V_g)$,[15] where C_g is the gate capacitance per unit area (ca. 7 nF $\cdot$ cm^{-2}); L and W, channel length and width, are about 2 and 5−10 μm, respectively; V_{sd} is 30 mV in our experiment. For the pristine graphene, the hole and electron mobilities are about 15 000 and 6700 cm^2 V^{-1} s^{-1}, respectively, which are consistent with the reported values.[7] For our N-doped graphene, the hole and electron mobilities are about 6000 cm^2 V^{-1} s^{-1}, higher than the values reported by nanoribbon,[17] graphene oxide, and graphene produced by CVD[15] or arc discharge.[41] Note that the electronic property of graphene annealed in N_2 after irradiation does not degrade, which is consistent with our previous conclusion that the defect of graphene could be restored after annealing in N_2 and the formation of the amorphous structure in graphene samples was avoided at the maximum fluence used in our experiment.[21] However, the conductance of the graphene annealed in NH_3 after irradiation is a few times lower compared to that of the pristine graphene, and it might be caused by the N atoms doping.

The atomic configuration and corresponding schematic band structures of the graphene illustrated in Figure 5 help to interpret the whole process of the experiment. The pristine graphene has 2D honeycomb atomic configuration and zero-gap band structure as shown in Figure 5a. After N^+-ion irradiation, the defects are induced as shown in Figure 5b. When annealing in NH_3, the last step to realize the change of Fermi energy in graphene,[31,42] NH_3 decomposes into atomic N, which can combine with the defect sites of the graphene as displayed by the right scheme in Figure 5c,[43] forming the most stable bonding against the high temperature based on the previous reports about the substitutional N-doping.[18−20,22,30]

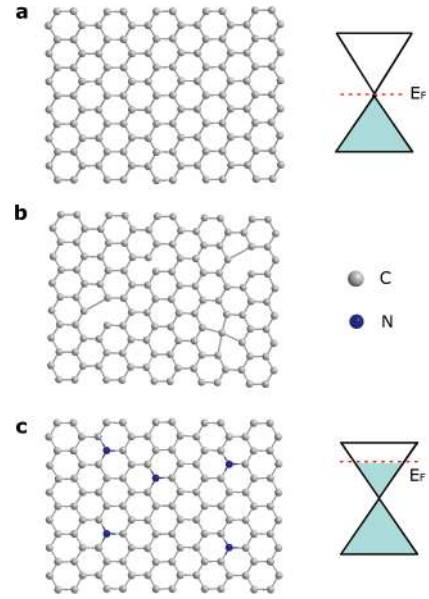

FIGURE 5. The atomic configuration and corresponding schematic band structures in the graphene sheet. (a) The atomic and band structures of the pristine graphene. (b) The representative vacancy defects of the irradiated graphene. (c) The atomic and band structures of the graphene annealed in NH_3 after irradiation. The doped graphene is formed by substituting some C atoms with N atoms.

After optimizing the fabrication process, for example, using shorter channel length, better contact metal, the device performances and doping efficiency will be greatly improved. The electronic properties of devices can also be exactly tuned by changing the doping parameters, such as dopant atoms, doping energy, and doses. The n-typed graphene together with the p-typed graphene can be used to fabricate p-n junction, which is the core of semiconductor devices, for example, junction transistor and integrated circuit. Our method provides a new approach for making N-doped graphene, which has promising prospect for producing graphene-based devices for multiple applications.

Acknowledgment. Jian Ru Gong sincerely thanks the financial support from Major National Basic Research Development Programs (No. 2009CB930200, 2011CB933401), Special Presidential Foundation of Chinese Academy of Sciences (No. O9312911ZX) and National Natural Science Foundations of China (No. Y0191111JJ, 21005023).

Supporting Information Available. Additional figures of effect of N_2 annealing on Raman spectra of graphene after irradiation and the transport data measured in vacuum for different graphene-based FETs are available free of charge via the Internet at http://pubs.acs.org.

REFERENCES AND NOTES

(1) Balandin, A. A.; Ghosh, S.; Bao, W.; Calizo, I.; Teweldebrhan, D.; Miao, F.; Lau, C. N. *Nano Lett.* **2008**, *8* (3), 902–907.
(2) Lee, C.; Wei, X.; Kysar, J. W.; Hone, J. *Science* **2008**, *321* (5887), 385–388.

DOI: 10.1021/nl103079j | *Nano Lett.* **2010,** *10,* 4975–4980

(3) Morozov, S. V.; Novoselov, K. S.; Katsnelson, M. I.; Schedin, F.; Elias, D. C.; Jaszczak, J. A.; Geim, A. K. *Phys. Rev. Lett.* **2008**, *100* (1), No. 016602.
(4) Chen, J.-H.; Jang, C.; Xiao, S.; Ishigami, M.; Fuhrer, M. S. *Nat. Nanotechnol.* **2008**, *3* (4), 206–209.
(5) Peirez-Jimeinez, A. n. J.; Sancho-Garciia, J. C. *J. Am. Chem. Soc.* **2009**, *131* (41), 14857–14867.
(6) Berger, C.; Song, Z.; Li, X.; Wu, X.; Brown, N.; Naud, C.; Mayou, D.; Li, T.; Hass, J.; Marchenkov, A. N.; Conrad, E. H.; First, P. N.; de Heer, W. A. *Science* **2006**, *312* (5777), 1191–1196.
(7) Novoselov, K. S.; Geim, A. K.; Morozov, S. V.; Jiang, D.; Zhang, Y.; Dubonos, S. V.; Grigorieva, I. V.; Firsov, A. A. *Science* **2004**, *306* (5696), 666–669.
(8) Geim, A. K.; Novoselov, K. S. *Nat. Mater.* **2007**, *6* (3), 183–191.
(9) Chen, Z.; Lin, Y.-M.; Rooks, M. J.; Avouris, P. *Physica E* **2007**, *40* (2), 228–232.
(10) Han, M. Y.; Özyilmaz, B.; Zhang, Y.; Kim, P. *Phys. Rev. Lett.* **2007**, *98* (20), 206805.
(11) Bai, J.; Zhong, X.; Jiang, S.; Huang, Y.; Duan, X. *Nat. Nanotechnol.* **2010**, *5* (3), 190–194.
(12) Giovannetti, G.; Khomyakov, P. A.; Brocks, G.; Kelly, P. J.; van den Brink, *J. Phys. Rev. B* **2007**, *76* (7), No. 073103.
(13) Rotenberg, E.; Bostwick, A.; Ohta, T.; McChesney, J. L.; Seyller, T.; Horn, K. *Nat. Mater.* **2008**, *7* (4), 258–259.
(14) Zhou, S. Y.; Gweon, G. H.; Fedorov, A. V.; First, P. N.; de Heer, W. A.; Lee, D. H.; Guinea, F.; Castro Neto, A. H.; Lanzara, A. *Nat. Mater.* **2007**, *6* (10), 770–775.
(15) Wei, D.; Liu, Y.; Wang, Y.; Zhang, H.; Huang, L.; Yu, G. *Nano Lett.* **2009**, *9* (5), 1752–1758.
(16) Ci, L.; Song, L.; Jin, C.; Jariwala, D.; Wu, D.; Li, Y.; Srivastava, A.; Wang, Z. F.; Storr, K.; Balicas, L.; Liu, F.; Ajayan, P. M. *Nat. Mater.* **2010**, *9* (5), 430–435.
(17) Wang, X.; Li, X.; Zhang, L.; Yoon, Y.; Weber, P. K.; Wang, H.; Guo, J.; Dai, H. *Science* **2009**, *324* (5928), 768–771.
(18) Xu, F.; Minniti, M.; Giallombardo, C.; Cupolillo, A.; Barone, P.; Oliva, A.; Papagno, L. *Surf. Sci.* **2007**, *601* (13), 2819–2822.
(19) Xu, F.; Minniti, M.; Barone, P.; Sindona, A.; Bonanno, A.; Oliva, A. *Carbon* **2008**, *46* (11), 1489–1496.
(20) Elman, B. S.; Dresselhaus, M. S.; Dresselhaus, G.; Maby, E. W.; Mazurek, H. *Phys. Rev. B* **1981**, *24* (2), 1027.
(21) Compagnini, G.; Giannazzo, F.; Sonde, S.; Raineri, V.; Rimini, E. *Carbon* **2009**, *47* (14), 3201–3207.
(22) Kim, K.-J.; Lee, H.; Choil, J.; Lee, H.; Jung, M. C.; Shin, H. J.; Kang, T.-H.; Kim, B.; Kim, S. *J. Phys.: Condens. Matter* **2010**, *22* (4), No. 045005.
(23) Tapasztó, L.; Dobrik, G.; Nemes-Incze, P.; Vertesy, G.; Lambin, P.; Biró, L. P. *Phys. Rev. B* **2008**, *78* (23), 233407.
(24) Ferrari, A. C. *Solid State Commun.* **2007**, *143* (1−2), 47–57.
(25) Kim, D. C.; Jeon, D.-Y.; Chung, H.-J.; YunSung Woo, Y. S.; Jai Kwang Shin, J. K.; Seo, S. *Nanotechnology* **2009**, *20* (37), 375703.
(26) Lucchese, M. M.; Stavale, F.; Ferreira, E. H. M.; Vilani, C.; Moutinho, M. V. O.; Capaz, R. B.; Achete, C. A.; Jorio, A. *Carbon* **2010**, *48* (5), 1592–1597.
(27) Ferrari, A. C.; Meyer, J. C.; Scardaci, V.; Casiraghi, C.; Lazzeri, M.; Mauri, F.; Piscanec, S.; Jiang, D.; Novoselov, K. S.; Roth, S.; Geim, A. K. *Phys. Rev. Lett.* **2006**, *97* (18), 187401.
(28) Krauss, B.; Lohmann, T.; Chae, D. H.; Haluska, M.; von Klitzing, K.; Smet, J. H. *Phys. Rev. B* **2009**, *79* (16), 165428.
(29) Zhang, Y.; Brar, V. W.; Wang, F.; Girit, C.; Yayon, Y.; Panlasigui, M.; Zettl, A.; Crommie, M. F. *Nat. Phys.* **2008**, *4* (8), 627–630.
(30) Tuinstra, F.; Koenig, J. L. Raman Spectrum of Graphite. *J. Chem. Phys.* **1970**, *53* (3), 1126–1130.
(31) Lin, Y.-C.; Lin, C.-Y.; Chiu, P.-W. *Appl. Phys. Lett.* **2010**, *96* (13), 133110.
(32) Tapaszt, L.; Dobrik, G.; Nemes-Incze, P.; Vertesy, G.; Lambin, P.; Bir, P. L. *Phys. Rev. B* **2008**, *78* (23), 233407.
(33) Feng, X.; Irle, S.; Witek, H.; Morokuma, K.; Vidic, R.; Borguet, E. *J. Am. Chem. Soc.* **2005**, *127* (30), 10533–10538.
(34) Wang, X.; Tabakman, S. M.; Dai, H. *J. Am. Chem. Soc.* **2008**, *130* (26), 8152–8153.
(35) Bradley, R. H.; Hellebust, S.; Daley, R. Presented at the 24th Biennial Conference of the American Carbon Society, Charleston, SC, July 11−16, 1999; 420−421.
(36) Guinea, F.; Katsnelson, M. I.; Geim, A. K. *Nat. Phys.* **2010**, *6* (1), 30–33.
(37) Compagnini, G.; Puglisi, O.; Foti, G. *Carbon* **1997**, *35* (12), 1793–1797.
(38) Ni, Z. H.; Wang, H. M.; Ma, Y.; Kasim, J.; Wu, Y. H.; Shen, Z. X. *ACS Nano* **2008**, *2* (5), 1033–1039.
(39) Gong, J.-R. *Small* **2010**, *6* (8), 967–973.
(40) Zheng, G.; Patolsky, F.; Cui, Y.; Wang, W. U.; Lieber, C. M. *Nat. Biotechnol.* **2005**, *23*, 1294–1301.
(41) Panchakarla, L. S.; Subrahmanyam, K. S.; Saha, S. K.; Govindaraj, A.; Krishnamurthy, H. R.; Waghmare, U. V.; Rao, C. N. R. *Adv. Mater.* **2009**, *21* (46), 4726–4730.
(42) Yang, Q.-H.; Hou, P.-X.; Unno, M.; Yamauchi, S.; Saito, R.; Kyotani, T. *Nano Lett.* **2005**, *5* (12), 2465–2469.
(43) Szczytkoa, J.; Juszyńskia, P.; Teligaa, L.; Stonertb, A.; Ratajczakb, R.; Kormanb, A.; Twardowskia, A. *Acta Phys. Pol., A* **2008**, *114* (5), 1387–1390.

DOI: 10.1021/nl103079j | *Nano Lett.* **2010,** *10,* 4975–4980